

Interweaving Chiral Spirals at finite quark density*

TORU KOJO

RIKEN BNL Research Center, Brookhaven National Laboratory, Upton,
NY-11973, USA

Faculty of Physics, University of Bielefeld, D-33501, Bielefeld, Germany

The interweaving chiral spirals (ICS), that is defined as superposition of differently oriented chiral spirals, is important for qualitative understandings of the intermediate quark density region as well as quantitative estimates of the Quarkyonic region. We discuss how to construct the ICS, taking the (2+1) dimensional Fermi system as an example. We postulate that the presence of the ICS would delay the occurrence of the chiral restoration as well as deconfinement phase transition, by tempering the growth of quark fluctuations.

PACS numbers: 12:38Aw, 11.30.Rd

1. Central Ideas: Qualitative Impacts of the ICS

Recently, it has been argued that there is a new state of QCD matter at high baryon density and low to intermediate temperatures [1] (Fig.1).

This novel state is called Quarkyonic matter, distinguished from nuclear matter by its bulk quantities such as pressure. The Fermi sea is mainly composed of quarks, not nucleons, in the region a little bit above $\mu_q \sim M_N/N_c \sim \Lambda_{\text{QCD}}$. This is because after the emergence of nucleons, a small change in μ_q rapidly enhances nucleon density, making strong short distance interactions among nucleons crucial. Thereby nucleons are not appropriate degrees of freedom to describe the bulk part of the Fermi sea – the quark picture is absolutely necessary to describe Quarkyonic matter.

Quarkyonic matter should be also distinguished from conventional deconfined quark matter by its thermal and Fermi surface excitations. The excitations are confined, even after quarks are released from nucleons. A proper understanding of confined excitations is a basic starting point for any

* Presented at “Three Days in Quarkyonic Island”, 19-21 May, 2011, Wroclaw, Poland.

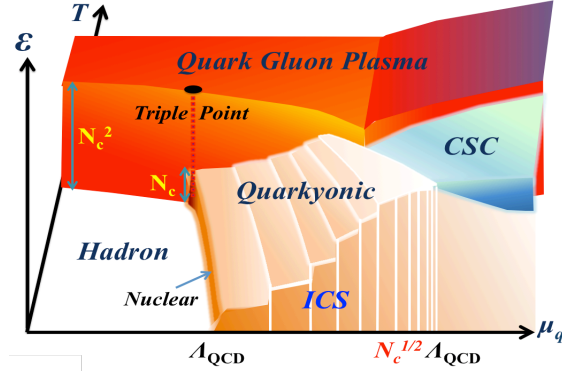


Fig. 1. A speculated QCD phase diagram.

discussions of phase structures, transport phenomena, and for construction of the effective Lagrangian.

One of the most relevant observations in Ref. [1] is that the scale for the formation of the quark Fermi sea, $\mu_q \sim \Lambda_{\text{QCD}}$, and that for the deconfinement of the excitations, $\mu_q \sim N_c^{1/(d-1)} \Lambda_{\text{QCD}}$ (d : spatial dimension), are conceptually different. The latter may be estimated by comparing quantum fluctuations of gluons with those of quarks near the Fermi surface. This observation was tested for (1+1) dimensional QCD, and it was argued that excitations are always confined¹ indendently of N_c , while the pressure is saturated by free quark contributions [2].

Now let us ask what happens to chiral symmetry. This issue is very important for qualitative understandings of the intermediate density region as well as *quantitative* estimates for the Quarkyonic region. Below we will argue that chiral symmetry is spontaneously *broken* by inhomogeneous chiral spirals, tempering the growth of the quark fluctuations at finite density.

Sometimes it is said that Quarkyonic matter is *defined* as a chiral symmetric confined matter, although chiral symmetry was *not* a primary issue in the original proposal of Ref. [1]. If one sticks to this definition, it might be very difficult to imagine the existence of Quarkyonic matter at $N_c = 3$. Indeed, once the quarks near the Fermi surface become gapless, it would largely enhance quark fluctuations in addition to the phase space enhancement at finite density. Recent results of the functional renormalization group application to the PNJL model for not very high density [3] presumably should be interpreted in this context.

A general tendency of model analyses, *without depending on whether models are confining or not*, suggests that the chiral restoration occurs

¹ In spatial one dimension, the phase space for quark fluctuations is always the same as vacuum case, so the confining force is never modified.

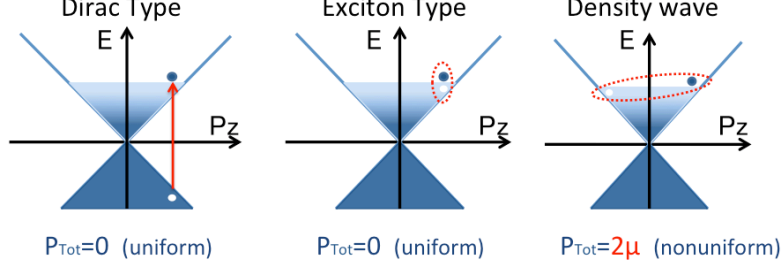


Fig. 2. Three types of chiral pairings.

shortly after the formation of the quark Fermi sea, or $p_F \sim \Lambda_{\text{QCD}}$ [4]. This trend may be understood by observing that the creation of anti-quarks, which are ingredients of the usual chiral condensate, costs more energy for the larger quark Fermi sea. This is so because the particle in the Dirac sea must go above the Fermi surface to avoid the Pauli-blocking (Fig.2).

At finite density, however, more proper ingredients of condensates are particle-holes near the Fermi surface. The excitations near the Fermi surface naturally have large momenta, $|\vec{p}| \sim \mu_q$, but they do not cost *additional* kinetic energy much, compared to the energy before excitations. Shown in Fig.2 are the exciton and density wave pairings.

In an exciton case, the total momentum of a pair is ~ 0 , but the relative momentum between a particle and a hole is $\sim 2\mu_q$. In a confining model, such a pairing accompanies a large string, costing large potential energy.

In a density wave case, while the total momentum of a pair is $\sim 2\mu_q$, a particle and a hole co-move without forming a large string. Thus the density wave pairing should be energetically favored compared to the exciton pairing. (Arguments based on confining model picture is useful but not indispensable, though. See below.)

Actually the chiral density wave solution can be always interpreted as the chiral spirals. A key observation is that once we have a condensation of a pair moving to, say, $+z$ -direction, there is also a pair moving to $-z$ direction. Mathematically, one can project out fermion components moving to $\pm z$ directions by operating the projection matrices [5],

$$\psi_{\pm} \equiv \frac{1 \pm \gamma_0 \gamma_z}{2} \psi. \quad (1)$$

Then we have two types of the chiral condensates,

$$\langle \bar{\psi}_- \psi_+ \rangle \sim \Delta e^{2i\mu_q z}, \quad \langle \bar{\psi}_+ \psi_- \rangle \sim \Delta e^{-2i\mu_q z}, \quad (2)$$

whose sum and difference give

$$\langle \bar{\psi} \psi \rangle \sim \Delta \cos(2\mu_q z), \quad \langle \bar{\psi} i \gamma_0 \gamma_z \psi \rangle \sim \Delta \sin(2\mu_q z), \quad (3)$$

with a fixed radius of Δ of the order Λ_{QCD}^3 . These condensates obviously break the chiral symmetry, translational invariance, rotational invariance, and the second condensate further breaks parity *locally*.

Here once again we emphasize that in the presence of the Fermi sea, large momenta naturally appear without costing much excitation energies, so one should not be surprised at the emergence of condensations with relatively large momenta. Indeed, analyses of both non-confining [6, 7, 8, 9] and confining models [5] suggest that the chiral spiral solution overtakes the homogeneous solution.

Rather a more nontrivial question is related to the fact that the chiral spiral must have a particular orientation. Let us ask: Can chiral pairs be formed in such a way to cover the entire Fermi surface, and can differently oriented chiral spirals be interweaved in a consistent way?

To answer to these questions will be very important for considerations about whether the chiral symmetry breaking may survive after taking the color superconductivity into account. If only single chiral spiral in one particular direction were possible, we could employ a less number of pairs for chiral condensations than we do for diquark condensations. If this would be the case, the color superconducting phase would overtake a single chiral spiral [7]. But instead we shall suggest a possibility that the ICS appears as far as the nonperturbative gluon exchange survives.

A possibility of the ICS has been qualitatively discussed in a confining model [10], although whole aspects about the ICS were not fully explored because of the technical difficulties in treating the deep infrared region of the gluon exchange. Actually, however, key aspects about the ICS may be extracted without using the confinement, and, in fact, are rather robust to the detailed behaviors in the deep infrared region.

Below we shortly highlight how to construct the ICS for the non-confining model in (2+1) dimensions, together with the parametric estimates of several effects. How to handle the corrections, relations with the previous works [8, 9], etc., have been comprehensively discussed in a recent paper [11], so an interested reader should consult it for details.

2. How to Construct the ICS in (2+1) dimensions

As an example of the ICS, we consider a (2+1) dimensional Fermi sea² at $T = 0$, purely because possible shapes of the Fermi surface are relatively simple. An extension of our treatments to higher dimensional systems are technically nontrivial but conceptually straightforward.

² Precisely speaking, in odd dimensional space-time, the chirality is not defined, so the terminology “chiral” spirals may be a little bit misleading. But the mechanism to generate spirals do not depend on this fact.

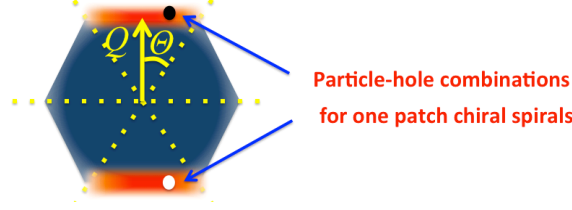


Fig. 3. A 3-patches = 6-wedges case.

We first divide the Fermi sea into $2N_p$ wedges (Fig.3). A wedge in one side of the Fermi sea and a wedge in the opposite side are regarded as a pair, and we call it one patch domain. We denote the height of each wedge as Q , and its open angle as $2\Theta = \pi/N_p$. Each patch will generate a single chiral spiral. The variables Q and Θ are variational parameters which will be optimized in such a way to minimize the total free energy.

Below we will use the canonical ensemble with specifying quark number density or p_F , because the presentation of ideas becomes simpler than the grand canonical case. Then the Fermi volume conservation can be used to rewrite Q as a function of p_F and Θ . In the canonical ensemble, our goal is to minimize the total energy³ by choosing the optimal value of Θ .

Essentially, the total energy and the shape of the Fermi surface will be determined by balancing the following energy costs and gains (Fig.4):

- (i) The kinetic energy cost arising from the deformation of the Fermi surface, which weakly depends upon the condensation effects. This contribution becomes dominant for large Θ .
- (ii) The energy gain in a single patch from the condensation effects. The condensation effects bend down the single particle dispersion. Then particles occupy smaller energy orbits, reducing the total single particle energy. In the following the quark mass gap will be denoted as M . This contribution is less sensitive to the angle Θ compared to other contributions.
- (iii) Coherent interactions among differently oriented chiral spirals (we call it inter-patch interaction) which cost energy. They originate from the condensation effects, so become less important as condensates get smaller. It becomes increasingly important for small Θ due to the enhanced number of inter-patch interactions.

³ At $T = 0$, the minimization of the free energy in the grand canonical ensemble is thermodynamically equivalent to the minimization of the total energy in the canonical ensemble.

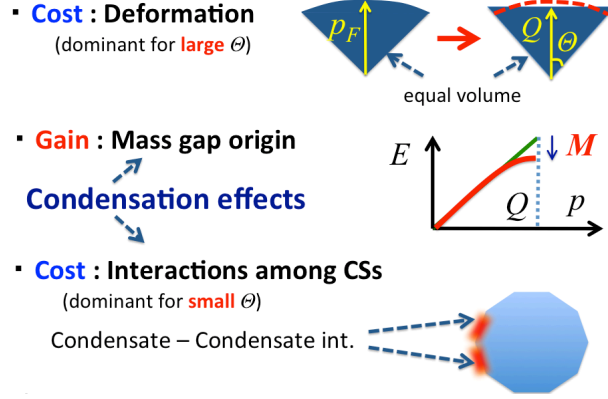


Fig. 4. The energy gains and costs.

Below we shall give estimates for these contributions, starting with the theoretically clean set up, that is, the leading order (LO) of the $1/N_c$ expansion and the high density expansion in powers of Λ_{QCD}/p_F . Although LO results are not directly applied to the phenomenologically interesting region, it is not difficult to specify which effects will grow at lower density, and how results will be modified qualitatively. Indeed, many features of the previous works [8, 9], which have been numerically done for relatively lower density, can be understood from this analytic framework.

For explicit estimates, it is indispensable to introduce models. In particular, the momentum dependence of the interaction strongly affects the estimate of the inter-patch interactions. We will explain the features of the model, then move to parametric estimates of several effects.

2.1. A model

In many studies of the intermediate density, typically the 4-Fermi interaction has been used, with the ultraviolet (UV) cutoff on the quark momenta. But this approach will be problematic when the quark Fermi momentum p_F becomes closer to the UV cutoff. Thus we have to use alternative descriptions at the intermediate density region. Our model is the following non-local 4-Fermi interaction,

$$\int d^3x (\bar{\psi}\psi(x))^2 \rightarrow \int dx_0 \int_{q,p,k} (\bar{\psi}(\vec{p} + \vec{q})\psi(\vec{p}))(\bar{\psi}(\vec{k})\psi(\vec{k} + \vec{q})) \theta_{p,k}, \quad (4)$$

where $\theta_{p,k} \equiv \theta(\Lambda_{\text{QCD}}^2 - (\vec{p} - \vec{k})^2)$, and momentum integration is for $\vec{q}, \vec{p}, \vec{k}$. The large- N_c QCD is mimicked as follows. The one-gluon exchange including non-perturbative effects are shown in Fig. 5(a). Its strength damps as

the momentum transfer becomes large. We roughly take into account this property by introducing a step function, $\theta(\Lambda_{\text{QCD}}^2 - (\vec{p} - \vec{k})^2)$, keeping the interaction strength constant.

In Fig. 5(b), we show the color line representation to illustrate how the one-gluon exchange interaction should be contracted into a four-Fermi type interaction. Taking into account features in Figs. 5(a) and 5(b), we arrive at a simple model described in Eq. (4) and Fig. 5(c).

The main consequence of our form factor treatments can be best seen in the Schwinger-Dyson or gap equations (See Fig. 5). We illustrate it for zero density case. After picking up a residue, we arrive at

$$M(\vec{p}) = \int \frac{d\vec{k}}{(2\pi)^2} \frac{M(\vec{k})}{2\epsilon(\vec{k})} \theta_{p,k} \cdot \left(\epsilon(\vec{k}) = \sqrt{M(\vec{k})^2 + \vec{k}^2} \right) \quad (5)$$

Note that because of $\theta_{p,k}$, the contributions to the mass gap $M(\vec{p})$ comes from the integral around \vec{p} . Putting in a different way, a particle with \vec{p} is affected by the condensate made of particles and anti-particles with momenta close to \vec{p} . So quark-condensate interactions are *local in momentum space*. Also it is clear that at very large $|\vec{p}|$, the integrand quickly damps, leading to small $M(\vec{p})$. The chiral restoration occurs for high energy excitations.

By applying this argument, one can derive several conclusions about finite density. The low energy excitations appear near the Fermi surface, so that the chiral symmetry is violated near the Fermi surface, but it is gradually restored in the region far from the Fermi surface.

Thanks to the locality in momentum space, the inter-patch interactions among condensates occur only if their momentum domains are close. In the construction of the ICS, this property is essential to restrict interactions among differently oriented chiral spirals only near the patch boundaries. If this locality is absent, inter-patch interactions would occur everywhere in the Fermi surface destroying the chiral spirals one another, and would reduce the quark mass gap considerably [9].

Now we are ready to give qualitative estimates of several contributions.

2.2. The energy cost: Deformation energy

The contribution (i) is rather easily estimated. In one wedge, Q is fixed by the Fermi volume conservation,

$$p_F^2 \Theta = Q^2 \tan \Theta, \quad (6)$$

and the difference between the Deformed Fermi sea and the spherical Fermi sea can be calculated as

$$\Delta \mathcal{E}_{\text{deform.}}(\Theta) \sim N_c \cdot p_F^3 \Theta^4 + O(\Theta^6), \quad (7)$$

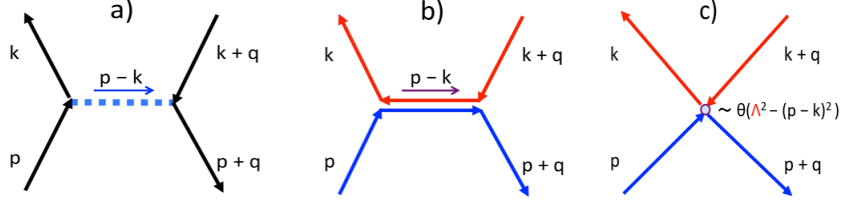


Fig. 5. (a) The non-perturbative gluon exchange which is supposed to damp quickly in the UV region. (b) The color line representation of the one-gluon exchange. (c) Our effective four-Fermi interaction including form factor effects.

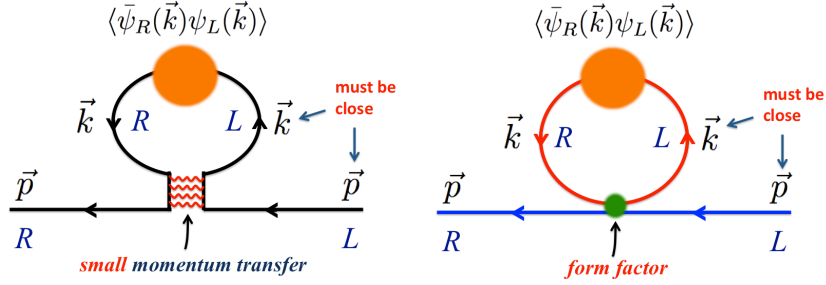


Fig. 6. The leading self-energy diagram at zero density. (Left) The diagram in terms of QCD dynamics with the Rainbow Ladder approximation. (Right) The corresponding diagram in our model.

where we have assumed $\Theta \ll 1$ and $M/p_F \ll 1$. Interestingly, Θ^2 term disappears after the subtraction of the spherical Fermi sea.

2.3. The energy gain: Single particle energy

The solution of the gap equation gives the mass gap, $M \sim \Lambda_{\text{QCD}}$, opened near the Fermi surface within distance of $\sim \Lambda_{\text{QCD}}$. On the other hand, quarks outside of this domain are not strongly affected by the condensates. Thus the energy reduction after summing up all patch contributions is

$$\Delta \mathcal{E}_{\text{cond.}}(\Theta) \sim N_c \cdot (-M) \times (\Lambda_{\text{QCD}} \cdot p_F \tan \Theta) \times N_p \sim -N_c \Lambda_{\text{QCD}}^2 p_F, \quad (8)$$

where $-M$ and $\Lambda_{\text{QCD}} \cdot p_F \tan 2\Theta$ characterizes the bending down of single particle energy, a number of particles acquiring the mass gap within a single patch, respectively. A sum of all patch contributions is approximately Θ independent, and does not play a relevant role in the optimization of Θ .

2.4. The energy cost: Inter-patch interactions among condensates

Since the single particle and the condensate interact only if their domains in momentum space are close one another, so interactions between differently oriented chiral spirals occur only near the patch boundaries. The strength of the interaction is proportional to M^2 . Taking into account the phase space where interactions occur, and counting a number of patch boudaries, we estimate the energetic cost as

$$\Delta\mathcal{E}_{\text{int.}}(\Theta) \sim N_c \cdot M^2 \Lambda_{\text{QCD}} \times N_p \sim N_c \Lambda_{\text{QCD}}^3 / \Theta. \quad (9)$$

Note that the contributions are proportional to $1/\Theta$, so the creation of condensates are not favored for very small Θ . Actually, near the patch boundaries the quark mass gap becomes effectively smaller.

2.5. The optimal value of Θ

Now we can optimize Θ by differentiating the total energy. Since the single particle contributions do not strongly depend on details of Θ , the optimal value of Θ is essentially determined by balancing the deformation energy and the inter-patch interaction energy:

$$\frac{1}{N_c} \frac{\partial}{\partial \Theta} (\Delta\mathcal{E}_{\text{deform.}} + \Delta\mathcal{E}_{\text{int.}}) \sim 4p_F^3 \Theta^3 - \frac{\Lambda_{\text{QCD}}^3}{\Theta^2} \sim 0, \quad (10)$$

which determines the optimal value of Θ as

$$\Theta \sim \left(\frac{\Lambda_{\text{QCD}}}{p_F} \right)^{3/5}. \quad (11)$$

Therefore, a number of chiral spirals, N_p , increases as density does. Since N_p is an integer, the phase transition occurs discontinuously.

With this value of Θ , the deformation and interaction energies are $\sim p_F^{3/5} \Lambda_{\text{QCD}}^{12/5}$, smaller than the single particle contribution, $\sim -p_F \Lambda_{\text{QCD}}^2$.

3. Summary

We have argued why the ICS is potentially relevant, and shown how to construct it by taking the (2+1) dimensional Fermi system as an example.

The chiral spirals is a mechanism that can generate the quark mass gap of $O(\Lambda_{\text{QCD}})$ even after the formation of the quark Fermi sea. We expect that the mass gap would temper the growth of the quark fluctuations near the Fermi surface, shifting chiral restoration and deconfinement lines to higher temperature and density than those predicted under the assumption of the homogeneous condensates.

We have argued the ICS only at $T = 0$, but for phenomenological applications to the RHIC low energy scan or future FAIR and NICA experiments, the extension of the present results to $T \neq 0$ are absolutely necessary. We expect that some qualitative changes occur at some temperature. Such an extension will be presented in near future.

Acknowledgments

The author thanks the organizers for their kind hospitality. Special thanks go to Y. Hidaka, K. Fukushima, L. McLerran, R.D. Pisarski, and A.M. Tsvelik with whom most of arguments presented here have been developed. He also acknowledges D. Blaschke, E.J. Ferrer, V. Incera, J.M. Pawłowski, A. Ohnishi, G. Torrieri for discussions during the workshop, and S. Carignano and M. Buballa for explaining their studies on the chiral crystals before the publication. He is supported by RIKEN-BNL Research Center and Humboldt foundation through its Sofja Kovalevskaja program.

REFERENCES

- [1] L. McLerran, R. D. Pisarski, Nucl. Phys. A **796** (2007) 83.
- [2] T. Kojo, [arXiv:1106.2187 [hep-ph]].
- [3] T. K. Herbst, J. M. Pawłowski and B. J. Schaefer, Phys. Lett. B **696** (2011) 58.
- [4] L. Y. Glozman, R. F. Wagenbrunn, Phys. Rev. D **77** (2008) 054027.
- [5] T. Kojo, Y. Hidaka, L. McLerran, R. D. Pisarski, Nucl. Phys. A **843** (2010) 37.
- [6] D. V. Deryagin, D. Y. Grigoriev, V. A. Rubakov, Int. J. Mod. Phys. A **7** (1992) 659.
- [7] E. Shuster, D. T. Son, Nucl. Phys. B **573** (2000) 434; B. Y. Park, M. Rho, A. Wirzba, I. Zahed, Phys. Rev. D **62** (2000) 034015.
- [8] D. Nickel, Phys. Rev. Lett. **103** (2009) 072301; Phys. Rev. D **80** (2009) 074025; S. Carignano, D. Nickel, M. Buballa, Phys. Rev. D **82** (2010) 054009.
- [9] R. Rapp, E. V. Shuryak, I. Zahed, Phys. Rev. D **63** (2001) 034008.
- [10] T. Kojo, R. D. Pisarski, A. M. Tsvelik, Phys. Rev. D **82** (2010) 074015.
- [11] T. Kojo, Y. Hidaka, K. Fukushima, L. McLerran, R. D. Pisarski, [arXiv:1107.2124 [hep-ph]].